

## COVID-19-associated brain abscess caused by *Trichosporon dohaense*: A case report and review of literature

Arghadip Samaddar<sup>a</sup>, Jyoti Diwakar<sup>a</sup>, Priya Krishnan<sup>a</sup>, HB Veena Kumari<sup>a</sup>, M Kavya<sup>a</sup>, Subhas Konar<sup>b</sup>, Dinesh A. Sharma<sup>c</sup>, BN Nandeesh<sup>d</sup>, Aditi Goyal<sup>d</sup>, S Nagarathna<sup>a,\*</sup>

<sup>a</sup> Department of Neuromicrobiology, National Institute of Mental Health and Neuro Sciences, Bengaluru, 560029, Karnataka, India

<sup>b</sup> Department of Neurosurgery, National Institute of Mental Health and Neuro Sciences, Bengaluru, 560029, Karnataka, India

<sup>c</sup> Department of Neuroimaging & Interventional Radiology, National Institute of Mental Health and Neuro Sciences, Bengaluru, 560029, Karnataka, India

<sup>d</sup> Department of Neuropathology, National Institute of Mental Health and Neuro Sciences, Bengaluru, 560029, Karnataka, India

### ARTICLE INFO

#### Keywords:

COVID-19

Brain abscess

*Trichosporon dohaense*

MALDI-TOF MS

Internal transcribed spacer

### ABSTRACT

We report the first case of Coronavirus Disease 2019 (COVID-19)-associated brain abscess caused by a rare *Trichosporon* species, *T. dohaense*. The patient was a known diabetic and had received systemic corticosteroids for the treatment of COVID-19. He underwent craniotomy and evacuation of abscess. The pus aspirate grew a basidiomycetous yeast, morphologically resembling *Trichosporon* species. The isolate was initially misidentified by VITEK® MS due to lack of mass spectral database of *T. dohaense*. Accurate identification was achieved by internal transcribed spacer-directed panfungal polymerase chain reaction. The patient had a favorable outcome following surgical intervention and antifungal therapy.

### 1. Introduction

Coronavirus Disease 2019 (COVID-19) pandemic caused by Severe Acute Respiratory Syndrome Coronavirus 2 (SARS-CoV-2) has a devastating impact on healthcare systems across the world. Recent studies indicate that COVID-19 patients are particularly vulnerable to a wide range of opportunistic fungal infections [1,2]. While *Aspergillus* spp., *Candida* spp., and *Mucormycetes* account for majority of these infections, other fungi, such as *Fusarium*, *Cryptococcus*, *Trichosporon*, *Histoplasma*, and *Coccidioides* are increasingly being reported [3,4]. It is still unclear whether fungal infections associated with COVID-19 are directly attributable to SARS-CoV-2 or a consequence of underlying factors such as neutropenia, poorly controlled diabetes, structural lung disease and/or other comorbidities, mechanical ventilation, and use of corticosteroids or immunomodulators for the treatment of COVID-19. *Trichosporon* species are yeast-like fungi that commonly colonize human skin and the respiratory and gastrointestinal tracts. However, they can cause invasive infections in immunocompromised hosts, particularly those with indwelling medical devices, cancer chemotherapy, broad-spectrum antibiotic therapy, hematologic malignancy, organ transplantation and prolonged intensive care unit (ICU) stay. To date, 16

species of *Trichosporon* have been identified as potential human pathogens, of which *T. asahii* accounts for majority of the invasive infections [5]. So far, eight cases of invasive trichosporonosis (7 cases of fungemia and 1 case of pneumonia) have been reported in COVID-19 patients, all of which are attributed to *T. asahii* [6,7]. Here, we report the first case of COVID-19-associated brain abscess caused by a *T. dohaense*, a rare *Trichosporon* species that was not previously known to cause central nervous system (CNS) infection.

### 2. Case presentation

A 55-year-old male presented to the Emergency department with headache and pain on right half of the face for one month. The headache was holocranial, mild and intermittent to begin with, which became severe, throbbing, continuous, and associated with right-sided tinnitus during the past 15 days. The symptoms were spontaneous in onset, not associated with nausea or vomiting and not relieved by medication. There was no history of fever, loss of consciousness or seizures. He was diagnosed with Coronavirus Disease 2019 (COVID-19) one and half months back and was treated with supplemental oxygen, remdesivir, methylprednisolone (16 mg/day x 1 week), azithromycin, doxycycline

; MALDI-TOF MS, Matrix-assisted laser desorption/ionization time-of-flight mass spectrometry.

\* Corresponding author.

E-mail address: [nagarathnachandrashekar@gmail.com](mailto:nagarathnachandrashekar@gmail.com) (S. Nagarathna).

<https://doi.org/10.1016/j.mmcr.2021.12.002>

Received 4 October 2021; Received in revised form 1 December 2021; Accepted 10 December 2021

Available online 16 December 2021

2211-7539/© 2021 The Author(s). Published by Elsevier B.V. on behalf of International Society for Human and Animal Mycology. This is an open access article

under the CC BY-NC-ND license (<http://creativecommons.org/licenses/by-nc-nd/4.0/>).

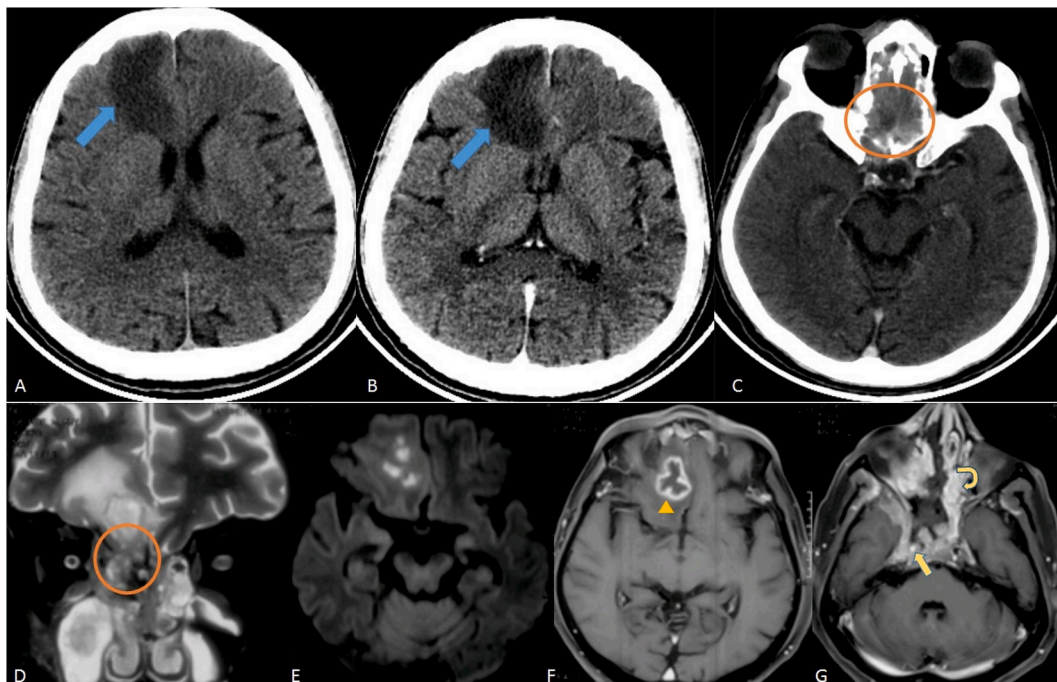


**Fig. 1.** Axial non-contrast (A) and contrast (B) CT brain at basifrontal level showing non-enhancing hypodensity (blue arrows) in right medial frontal lobe extending till the margins of right frontal horn. Contrast CT brain axial section (C) showing enhancing soft tissue mass (circled) in ethmoidal air cells. MRI Brain T2w coronal section (D) showing mixed signal intensity lesion involving ethmoidal air cells, extending across the cribriform plate (circled) to involve right basifrontal lobe with associated edema in the involved parenchyma. Diffusion weighted axial section (E) showing foci of diffusion restriction within gyrus rectus and pars orbitalis. Axial T1 postcontrast sections (F, G) showing peripheral ring-enhancing lesion in right frontal lobe (arrow head) with thick enhancing soft tissue mass involving paranasal sinuses (curved arrow), infiltrating posteriorly to involve cavernous sinuses and anterior part of the carotid canal encasing bilateral internal carotid arteries. Right ICA shows loss of flow void suggestive of thrombosis (blue arrow), thus representing angioinvasive nature of the lesion. (For interpretation of the references to colour in this figure legend, the reader is referred to the Web version of this article.)

and ivermectin. He was a known diabetic on insulin and oral hypoglycemic drugs for 15 years. He was a known hypertensive and on regular medicine for five years. On admission (day 0), the patient was alert, conscious and oriented and vitals were stable. Neurological examination revealed tenderness along the ophthalmic and maxillary divisions of right trigeminal nerve, restriction of lateral movement of the right eye and right-sided conductive hearing loss. There were no sensory or motor deficits and no meningeal or cerebellar signs. Superficial and deep tendon reflexes were preserved. Ocular examination showed right-sided conjunctival chemosis, lid edema, esotropia, ptosis and proptosis. Visual acuity was normal (6/6) in both the eyes. Rest of the systems was within normal limits. The hematological profile showed anaemia (Hb = 9.6 g/dL [normal: 13–17 g/dL]); RBC count =  $3.67 \times 10^6/\mu\text{l}$  [Normal: 4.5–5.5

$\times 10^6/\mu\text{l}$ ] and low hematocrit (30.9% [Normal: 40–50%]). Biochemical investigations revealed hyperglycemia (random blood glucose = 151 mg/dL [Normal: 70–140 mg/dL]), elevated HbA1c (7.8% [Normal: 4.0–5.7%]), hypoalbuminemia (serum albumin = 2.9 g/dL [Normal: 3.5–5.2 g/dL]), low albumin:globulin ratio (0.9 [Normal: 1.2–2.5]), hyponatremia ( $\text{Na}^+$  = 128.6 mmol/L [Normal: 136–145 mmol/L]), and hyperkalemia ( $\text{K}^+$  = 5.28 mmol/L [Normal: 3.5–5.1 mmol/L]). Coagulation profile, liver enzymes and renal function tests were within normal limits. Urinalysis was negative for ketone bodies. Contrast enhanced computed tomography (CECT) of brain and paranasal sinuses (day 0) revealed hypodensity in right medial frontal lobe extending till the margins of right frontal horn with ethmoidal sinusitis, erosion of the cribriform plate and intracranial extension (Fig. 1A–C). Magnetic

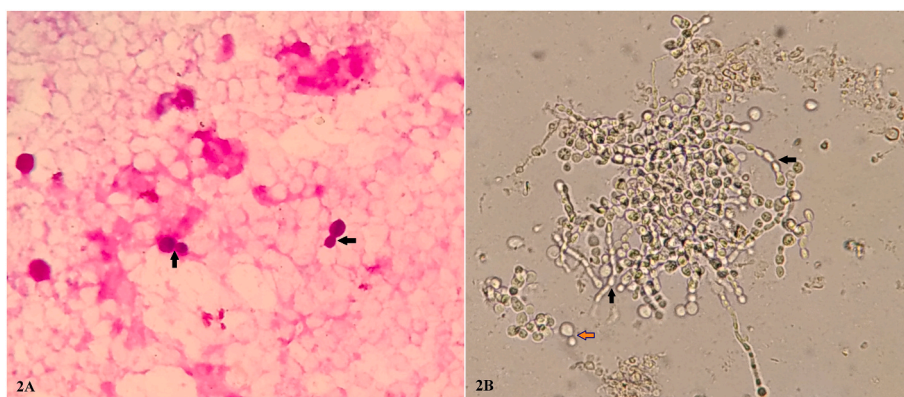


**Fig. 2.** Microscopic examination of pus. (A) Gram positive oval to ellipsoidal broad-based budding yeast cells (black arrows; x1000) (B) Numerous broad-based budding yeast cells (orange arrow) with pseudohyphae and arthroconidia (black arrows; x400) [A: Gram stain; B: 10% KOH mount]. (For interpretation of the references to colour in this figure legend, the reader is referred to the Web version of this article.)

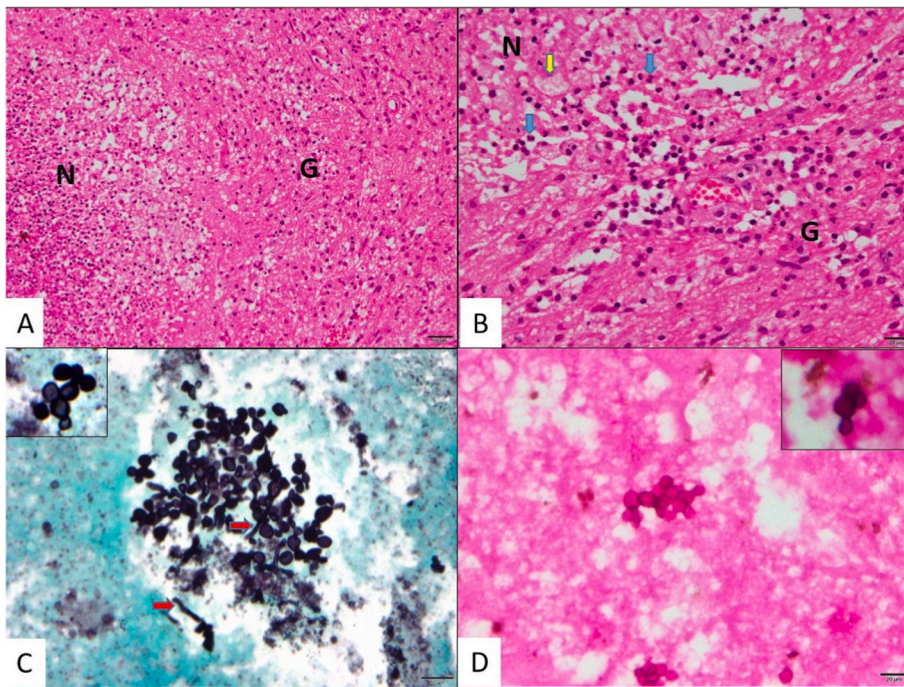


**Fig. 3.** Histopathological examination showing suppurative granulomatous lesion with fungal elements. **A** (x100) Zonation in the abscess wall with central necrotic area (N) surrounded by granulation tissue (G). **B** (x200) Foamy macrophages (yellow arrow) and polymorphs (blue arrows) in the necrotic area (N) with surrounding granulation tissue (G) containing inflammatory cells, newly formed blood vessels and fibroblastic proliferation. Cell block prepared from abscess fluid reveals numerous budding yeast cells (**C**, **D** inset; x400) and occasional hyphae (**C**, red arrows; x200). [**A**, **B**: Hematoxylin & Eosin, **C**: Grocott Gomori Methanamine Silver, **D**: Periodic acid Schiff (Scale bars- 50 μm)]. (For interpretation of the references to colour in this figure legend, the reader is referred to the Web version of this article.)

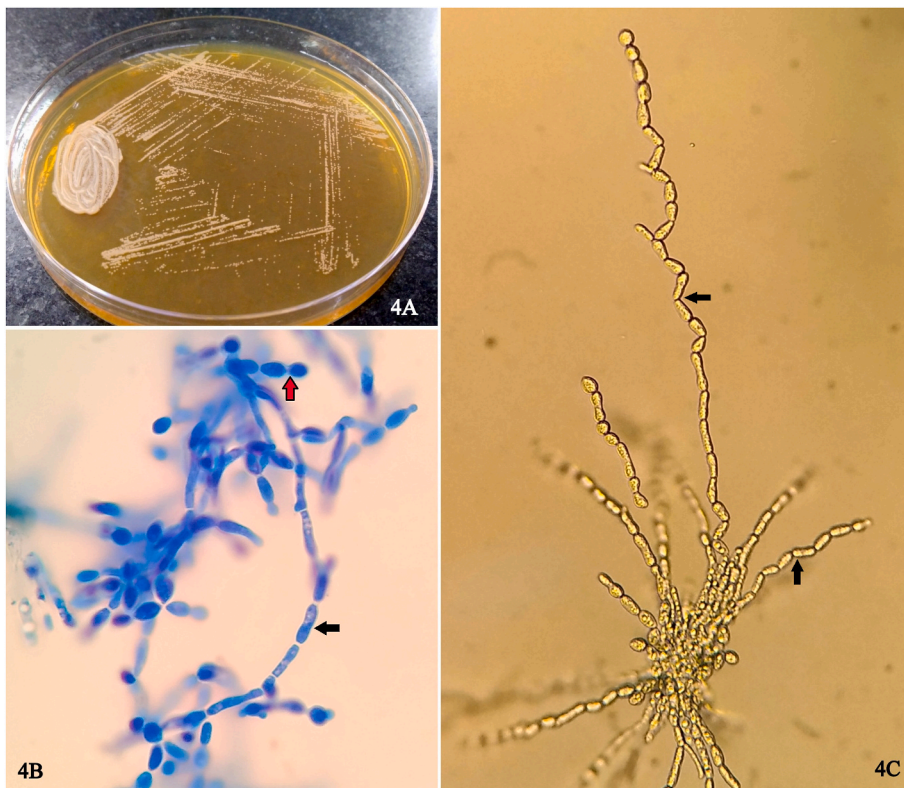


**Fig. 4.** Colony characteristics and microscopic morphology of *T. dohaense*. **(A)** Slow-growing, smooth, creamy, mucoid colonies of *T. dohaense* on SDA, after 72 h of incubation at 37 °C. **(B)** LPCB mount showing globose to ellipsoidal yeast cells with polar budding on a broad base (red arrow; x1000) and cylindrical variable sized arthroconidia (black arrow; x1000). **(C)** Dalmal culture on cornmeal agar showing extensive hyphae and cylindrical arthroconidia of variable size (x400). (For interpretation of the references to colour in this figure legend, the reader is referred to the Web version of this article.)

resonance imaging (MRI) of brain (day 0) revealed peripheral ring-enhancing lesions in the right frontal lobe with thick enhancing soft tissue mass involving the parasal sinuses, cavernous sinuses and encasing bilateral internal carotid arteries (ICA). There was thrombosis of the right ICA, indicating angioinvasive nature of the lesion (Fig. 1D–G). Based on the clinical and radiological findings, a diagnosis of right frontal brain abscess of infective etiology was established. The

patient underwent right frontal craniotomy and evacuation of pus (day +1). The abscess cavity contained yellowish-brown granular pus, surrounded by friable white capsule. The abscess was evacuated and a subgaleal drain was placed. The pus aspirate was sent for microbiological and histopathological examination (day +1). Gram staining of pus revealed Gram positive oval to ellipsoidal, broad-based budding yeast cells (Fig. 2A). Ten per cent potassium hydroxide (KOH) mount showed

**Table 1**Summary of infections caused by *Trichosporon dohaense* from 2009 to 2021.

Isolate No.	Reference (Year)	GenBank Accession No. (ITS)	Patient demographics		Clinical specimen	Infection	Antifungal therapy	Outcome
			Patient origin	Age/Gender				
Myco 643	Taj-Aldeen et al. (2009) [8]	FJ228476	Qatar	70/F	Toenail	Onychomycosis	Not known	Not known
Myco 194	Taj-Aldeen et al. (2009) [8]	FJ228474	Bangladesh	41/M	Catheter	Catheter-site infection	Not known	Not known
Myco 483	Taj-Aldeen et al. (2009) [8]	FJ228475	India	34/M	Skin scraping	Tinea pedis	Oral TRB + topical ECO + Whitfield's ointment	Recovered
AUMC 10212	Abdel-Sater et al. (2016) [9]	KU200438	Egypt	40/F	Fingernail	Onychomycosis	Not known	Not known
10PU193	Yu et al. (2018) [10]	MG857685	China	56/M	Blood	Fungemia	Not given	LFU
12ZZ130	Yu et al. (2018) [10]	MG857710	China	81/F	CVC and blood	CLABSI	IV FLC	LFU
Isolate 1	Mohanty et al. (2020) [11]	MN796087	India	25/M	Blood	Fungemia	LAMB	Died
P103	Present case (2021)	OK090936	India	55/M	Pus	Brain abscess	LAMB, then switched to POS	Recovered

TRB, terbinafine; ECO, econazole; FLC, fluconazole; LAMB, liposomal amphotericin B; POS, posaconazole; CVC, central venous catheter; CLABSI, central line-associated bloodstream infection; IV, intravenous; LFU; lost to follow-up.

numerous oval, budding yeast cells with pseudohyphae and arthroconidia (Fig. 2B). Ziehl-Neelsen staining did not show acid-fast bacilli. Histopathological examination demonstrated numerous budding yeast cells with occasional hyphae in the background of a central necrotic area composed of polymorphs and foamy macrophages, surrounded by granulation tissue containing inflammatory cells, newly formed blood vessels and fibroblasts (Fig. 3). Blood and urine cultures were sterile. The pus aspirate was inoculated on routine bacteriological culture media and Sabouraud dextrose agar (SDA) with and without 0.01% cycloheximide, and incubated at 25 °C and 37 °C. There was no bacterial growth after 48 h of aerobic and anaerobic incubation. Fungal culture on SDA showed slow-growing, smooth, creamy, mucoid colonies after 72 h of incubation (day +4) (Fig. 4A). Microscopic examination revealed globose to ellipsoidal yeast cells with polar or occasionally lateral budding on a broad base. There were occasional pseudohyphae and cylindrical arthroconidia of variable size (Fig. 4B). Extensive hyphae and arthroconidia were observed in Dalmau culture on cornmeal agar (Fig. 4C). On the basis of colony characteristics, microscopic morphology, positive urea hydrolysis test and failure to grow in 0.01% cycloheximide, a presumptive identification of *Trichosporon* spp. was made (day +6). The isolate was identified as *T. ovoides*/*T. asteroides*, with confidence value of 50/50 by matrix-assisted laser desorption/ionization time-of-flight mass spectrometry (MALDI-TOF MS) (VITEK® MS, bioMérieux, Marcy l'Etoile, France). To confirm the species, genomic DNA of the isolate was extracted and polymerase chain reaction (PCR) amplification of the internal transcribed spacer (ITS) region and large subunit (LSU) ribosomal RNA gene was performed using primer pairs ITS1/ITS4 and NL1/NL4, respectively. The sequences were compared with those in the GenBank database using nucleotide Basic Local Alignment Search Tool (BLASTn). The ITS and LSU sequences of the isolate showed 99.8% and 99.7% similarity with *Trichosporon dohaense* strains CDCF2072 and 12ZZ130 (GenBank accession numbers MN809435 and MG857792), respectively. The sequences were deposited in the GenBank database and published in the National Center for Biotechnology Information (NCBI) database on September 20, 2021, under the name *Trichosporon dohaense* isolate P103 with accession numbers OK090936 (ITS) and OK135942 (LSU). In vitro antifungal susceptibility testing (AFST) was performed by broth microdilution method, according to the Clinical and Laboratory Standards Institute (CLSI) document M38-A2. The minimum inhibitory concentration (MIC) values of amphotericin B (AMB), fluconazole (FLC), voriconazole (VRC), posaconazole (POS), and 5-flucytosine (5FC) were 1 µg/mL, 16 µg/mL, 0.125 µg/mL, 0.25 µg/mL and 8 µg/mL, respectively. Postoperatively (day +1), the patient was advised intravenous (IV) liposomal

amphotericin B (LAMB) 10 mg/kg/day in 5% dextrose over 6 h for two weeks, ceftriaxone 1 gm IV twice a day for three days, amikacin 750 mg IV once a day for three days and metronidazole 500 mg IV thrice a day for three days. Human Actrapid (short-acting human insulin; 40 IU/ml) was administered subcutaneously as per sliding scale, along with strict glycemic monitoring. The patient was kept under observation in neurosurgery recovery ward for 48 h and then, shifted to another government hospital for further management (day +4). Due to non-availability of LAMB, the antifungal therapy was switched to oral posaconazole (2 × 300 mg on day 1, then 300 mg/day from day 2) on day +6. There was marked clinical and radiological improvement after 10 days. He was discharged from the hospital (day +18) with oral posaconazole for six months and advised to attend Neurosurgery outpatient department after three months for follow-up.

### 3. Discussion

We report the first case of COVID-19 associated brain abscess caused by *T. dohaense* in a diabetic patient. To our knowledge, this is also the first case of brain abscess caused by this rare *Trichosporon* species. So far, only seven cases of infection (4 cases of superficial infections, 2 cases of fungemia and 1 catheter-associated infection) caused by this fungus have been reported in literature (Table 1) [8–11].

*Trichosporon* species are yeast-like fungi belonging to the phylum *Basidiomycota*. They can cause a wide spectrum of diseases, ranging from superficial infection (white piedra) in immunocompetent individuals to fungemia and invasive trichosporonosis in immunocompromised hosts [5]. Out of 16 *Trichosporon* species implicated in human infections, six are of major clinical relevance, including *T. asahii*, *T. asteroides*, *T. cutaneum*, *T. inkin*, *T. mucoides* and *T. ovoides*. Others such as *T. japonicum*, *T. jirovecii*, *T. dermatis*, *T. montevidense*, *T. coremiiforme*, *T. domesticum*, *T. faecale*, *T. loubieri*, *T. dohaense*, and *T. mycotxinivorans* rarely cause human disease [5,8]. *T. dohaense* was first described in 2009 by Taj-Aldeen, Meis & Boekhout as a cause of superficial infections in immunocompromised patients in Qatar. It is a holotype strain, belonging to the *Ovoides* clade and is a sister species to *T. coremiiforme* [8]. While there are reports of CNS infection caused by *T. asahii*, *T. inkin* and *T. cutaneum* [12], brain abscess due to *T. dohaense* have not yet been reported.

Trichosporonosis is an endogenous disease as the fungus constitutes part of the human skin, respiratory and digestive tract microbiome [13]. The risk factors for invasive trichosporonosis in COVID-19 patients are similar to those well described in other clinical contexts, including hematologic malignancies, solid tumors, neutropenia, HIV/AIDS,

**Table 2**  
Antifungal susceptibility profile of clinical isolates of *Trichosporon dohaense* (2009–2021).

Isolate No.	Reference (Year)	Country	MIC (µg/mL)						
			AMB	FLC	ITC	VRC	POS	ISA	5FC
Myc0 643	Taj-Aldeen et al. (2009) [8]	Qatar	0.5–1	1–4	0.031–0.25	0.016–0.25	0.031–0.125	0.063–0.25	–
Myc0 194	Taj-Aldeen et al. (2009) [8]	Qatar							
Myc0 483	Taj-Aldeen et al. (2009) [8]	Qatar							
10PU193	Yu et al. (2018) [9]	China	1	8	0.5	0.25	0.25	–	4
12ZZ130	Yu et al. (2018) [9]	China	1	16	0.5	1	0.5	–	4
Isolate 1	Mohanty et al. (2020) [11]	India	1	–	–	–	–	–	–
P103	Present case (2021)	India	1	16	–	0.125	0.25	–	8

AMB, amphotericin B; FLC, fluconazole; ITC, itraconazole; POS, posaconazole; ISA, isavuconazole; 5FC, 5-flucytosine.

\*AFST results are not available for the isolate AUMC 10212, described by Abdel-Sater et al. (2016).

corticosteroid use, poorly controlled diabetes, use of central venous catheters, and renal dysfunction. Prolonged antimicrobial selection pressure, as happens during COVID-19 treatment, may favour overgrowth of *Trichosporon* spp. and subsequent colonization, which together with SARS-CoV-2 mediated immune dysregulation can lead to invasive trichosporonosis [14]. Though corticosteroid therapy has shown survival benefit in moderate to severe COVID-19, their prolonged use in high-dose may serve as a double-edged sword and have detrimental effects. COVID-19 itself causes immunosuppression through reduction and functional exhaustion of CD4<sup>+</sup> and CD8<sup>+</sup> T cells, which together with underlying diabetes and immunosuppressive action of steroids facilitate infections by opportunistic pathogens, including *Candida* and *Trichosporon* [15,16]. The present case had right-sided facial pain and proptosis with CECT findings suggestive of ethmoidal sinusitis, erosion of cribriform plate and intracranial extension. These indicate that immune dysregulation, along with underlying diabetes and intense dysbiosis and immunosuppression secondary to COVID-19 treatment might have facilitated colonization of the paranasal sinuses with *T. dohaense*, leading to sinusitis and subsequent intracranial extension to involve the frontal lobe.

Accurate identification of *T. dohaense* is important for initiation of appropriate antifungal therapy. *T. dohaense* is morphologically indistinguishable from other *Trichosporon* species and can easily be misidentified as *Candida* by conventional methods like CHROMagar and VITEK 2 YST [8,10]. Though MALDI-TOF MS serves as a promising tool for routine identification of most *Trichosporon* spp., the mass spectral data of *T. dohaense* are not represented in VITEK® MS (bioMérieux, Marcy l'Etoile, France) database, and therefore, our isolate was misidentified as *T. ovoides*/*T. asteroides*. However, Bruker Autoflex Speed (Bruker Daltonics, Bremen, Germany) contains the mass spectral data of *T. dohaense* and can reliably identify it [10]. Sequencing-based platforms targeting the ITS (ITS1-5.8S-ITS2) and LSU regions of fungal DNA have high discriminatory power and can provide accurate identification to the species level [8,17,18].

At present, there are no established minimum inhibitory concentration (MIC) breakpoints for antifungal drugs against *Trichosporon* spp. and hence, it is difficult to precisely confirm their susceptibility to these agents. However, AFST can be a useful guide for choosing appropriate antifungal therapy. *Trichosporon* spp. are inherently resistant to echinocandins and demonstrate variable MICs for fluconazole [5,12]. Though most *Trichosporon* spp. show high MICs for amphotericin B, *T. dohaense* has consistently demonstrated low MICs (0.5–1 µg/mL) for all isolates tested [8,10,11], including the present one. Among the newer triazoles, itraconazole, voriconazole, and posaconazole exhibit potent *in vitro* activity against *T. dohaense* [8,10], as observed with our isolate. Table 2 summarizes the AFST results of all clinical isolates of *T. dohaense* reported to date.

To our knowledge, the present report describes the first case of invasive infection caused by *T. dohaense*, which was successfully treated with antifungal drugs. Invasive trichosporonosis carries a high mortality rate (40–60%), despite antifungal therapy [5,19]. In absence of randomised trials and clinical breakpoints, recommendations for antifungal

therapy are based on *in vitro* studies and case series. Several studies have shown azole-based therapy to be superior to polyene-based therapy for the treatment of invasive trichosporonosis. Azole-polyene combination therapy has no advantage over azole monotherapy [12,18,20]. According to the Global guideline for the diagnosis and management of rare yeast infections issued by European Confederation of Medical Mycology (ECMM) in co-operation with International Society for Human and Animal Mycology (ISHAM) and American Society for Microbiology (ASM), treatment of invasive trichosporonosis should consist of either voriconazole or posaconazole for a duration of 4–6 weeks, or until radiological resolution (moderate recommendation) [18].

To conclude, *T. dohaense* is an emerging opportunistic fungal pathogen that can cause invasive infections, particularly in the context of COVID-19. The variable MICs for antifungal agents exhibited by this species highlight the importance of accurate identification for initiation of appropriate antifungal therapy. The currently available conventional systems and VITEK® MS are not reliable enough to identify correctly all the clinically relevant *Trichosporon* species and therefore, ITS-directed panfungal PCR should be performed for all *Trichosporon* isolates showing low confidence value by MALDI-TOF MS. An early diagnosis together with appropriate antifungal therapy can improve the outcomes in such cases.

#### Declaration of competing interest

The authors have no conflicts of interest to declare.

#### Acknowledgements

The authors are thankful to the National Fungal Culture Collection of India (NFCCI), Biodiversity and Paleobiology Group, MACS – Agharkar Research Institute, Pune, India, for molecular identification of the fungal isolate.

#### References

- [1] M. Hoenigl, Invasive Fungal Disease complicating COVID-19: when it rains it pours, Clin. Infect. Dis. (2020), <https://doi.org/10.1093/cid/ciaa1342>.
- [2] T.M. Rawson, R.C. Wilson, A. Holmes, Understanding the role of bacterial and fungal infection in COVID-19, Clin. Microbiol. Infect. 27 (2021) 9–11, <https://doi.org/10.1016/j.cmi.2020.09.025>.
- [3] J. Diwakar, A. Samaddar, S.K. Konar, M.D. Bhat, E. Manuel, H.B. Veenakumari, et al., First report of COVID-19-associated rhino-orbito-cerebral mucormycosis in pediatric patients with type 1 diabetes mellitus, J. Mycol. Med. 31 (2021) 101203, <https://doi.org/10.1016/j.mycmed.2021.101203>.
- [4] J.P. Gangneux, M.E. Bounoux, E. Dannaoui, M. Cornet, J.R. Zahar, Invasive fungal diseases during COVID-19: we should be prepared, J. Mycol. Med. 30 (2020) 100971, <https://doi.org/10.1016/j.mycmed.2020.100971>.
- [5] A.L. Colombo, A.C. Padovan, G.M. Chaves, Current knowledge of *Trichosporon* spp. and trichosporonosis, Clin. Microbiol. Rev. 24 (2011) 682–700, <https://doi.org/10.1128/CMR.00003-11>.
- [6] G.A. Ali, A. Husain, H. Salah, W. Goravey, *Trichosporon asahii* fungemia and COVID-19 co-infection: an emerging fungal pathogen; case report and review of the literature, IDCases 25 (2021), e01244, <https://doi.org/10.1016/j.idcr.2021.e01244>.

- [7] G. Segrelles-Calvo, G.R.S. Araújo, E. Llopis-Pastor, S. Frasés, *Trichosporon asahii* as cause of nosocomial pneumonia in patient with COVID-19: a triple Co-infection, *Arch. Bronconeumol.* 57 (Suppl 2) (2021) 46–48, <https://doi.org/10.1016/j.arbres.2020.11.007>.
- [8] S.J. Taj-Aldeen, N. Al-Ansari, S. El Shafei, J.F. Meis, I. Curfs-Breuker, B. Theelen, et al., Molecular identification and susceptibility of *Trichosporon* species isolated from clinical specimens in Qatar: isolation of *Trichosporon dohaense* Taj-Aldeen, Meis & Boekhout sp. Nov, *J. Clin. Microbiol.* 47 (2009) 1791–1799, <https://doi.org/10.1128/JCM.02222-08>.
- [9] M.A. Abdel-Sater, A.A. Moubasher, Z. Soliman, Identification of three yeast species using the conventional and internal transcribed spacer region sequencing methods as first or second global record from human superficial infections, *Mycoses* 59 (2016) 652–661, <https://doi.org/10.1111/myc.12520>.
- [10] S.Y. Yu, L.N. Guo, M. Xiao, T. Kudinha, F. Kong, H. Wang, et al., *Trichosporon dohaense*, a rare pathogen of human invasive infections, and literature review, *Infect. Drug Resist.* 11 (2018) 1537–1547, <https://doi.org/10.2147/IDR.S174301>.
- [11] A. Mohanty, S. Meena, U.K. Nath, A. Bakliwal, N. Kaistha, P. Gupta, *Trichosporon dohaense* causing life-threatening fungemia in acute leukemia: first case report from India, *Indian J. Pathol. Microbiol.* 64 (2021) 619–621, [https://doi.org/10.4103/IJPM.IJPM\\_185\\_20](https://doi.org/10.4103/IJPM.IJPM_185_20).
- [12] J.N. de Almeida Júnior, C. Hennequin, Invasive *Trichosporon* infection: a systematic review on a Re-emerging fungal pathogen, *Front. Microbiol.* 7 (2016) 1629, <https://doi.org/10.3389/fmicb.2016.01629>.
- [13] O. Cho, M. Matsukura, T. Sugita, Molecular evidence that the opportunistic fungal pathogen *Trichosporon asahii* is part of the normal fungal microbiota of the human gut based on rRNA genotyping, *Int. J. Infect. Dis.* 39 (2015) 87–88, <https://doi.org/10.1016/j.ijid.2015.09.009>.
- [14] J. Nobrega de Almeida Jr., L. Moreno, E.C. Francisco, G. Noronha Marques, A. V. Mendes, M.G. Barberino, et al., *Trichosporon asahii* superinfections in critically ill COVID-19 patients overexposed to antimicrobials and corticosteroids, *Mycoses* 64 (2021) 817–822, <https://doi.org/10.1111/myc.13333>.
- [15] A. Arastehfar, A. Carvalho, M.H. Nguyen, M.T. Hedayati, M.G. Netea, D.S. Perlin, et al., COVID-19-Associated candidiasis (CAC): an underestimated complication in the absence of immunological predispositions? *J. Fungi.* 6 (2020) 211, <https://doi.org/10.3390/jof6040211>.
- [16] J.Y. Rodriguez, P. Le Pape, O. Lopez, K. Esquea, A.L. Labiosa, C. Alvarez-Moreno, *Candida auris*: a latent threat to critically ill patients with COVID-19, *Clin. Infect. Dis.* (2020), <https://doi.org/10.1093/cid/ciaa1595>.
- [17] T. Sugita, A. Nishikawa, R. Ikeda, T. Shinoda, Identification of medically relevant *Trichosporon* species based on sequences of internal transcribed spacer regions and construction of a database for *Trichosporon* identification, *J. Clin. Microbiol.* 37 (1999) 1985–1993, <https://doi.org/10.1128/JCM.37.6.1985-1993.1999>.
- [18] S.C. Chen, J. Perfect, A.L. Colombo, O.A. Cornely, A.H. Groll, D. Seidel, et al., Global guideline for the diagnosis and management of rare yeast infections: an initiative of the ECMM in cooperation with ISHAM and ASM, *Lancet Infect. Dis.* (2021), [https://doi.org/10.1016/S1473-3099\(21\)00203-6](https://doi.org/10.1016/S1473-3099(21)00203-6).
- [19] S.Y. Ruan, J.Y. Chien, P.R. Hsueh, Invasive trichosporonosis caused by *Trichosporon asahii* and other unusual *Trichosporon* species at a medical center in Taiwan, *Clin. Infect. Dis.* 49 (2009) e11–e17, <https://doi.org/10.1086/599614>.
- [20] Y. Liao, X. Lu, S. Yang, Y. Luo, Q. Chen, R. Yang, Epidemiology and outcome of *Trichosporon* fungemia: a review of 185 reported cases from 1975 to 2014, *Open Forum Infect. Dis.* 2 (2015) ofv141, <https://doi.org/10.1093/ofid/ofv141>.